Evidence for absence of latch-bridge formation in muscular saphenous arteries

**Shaojie Han,[2] John E. Speich,[3] Thomas J. Eddinger,[4] Krystina M. Berg,[1]
Amy S. Miner,[1] Chris Call,[3] and Paul H. Ratz[1]**

[1]*Departments of Biochemistry and Pediatrics,* [2]*Department of Physiology,* [3]*Department of Mechanical
Engineering, Virginia Commonwealth University School of Medicine, Richmond, Virginia; and*
[4]*Department of Biological Sciences, Marquette University, Milwaukee, Wisconsin*

Han, Shaojie, John E. Speich, Thomas J. Eddinger, Krystina
M. Berg, Amy S. Miner, Chris Call, and Paul H. Ratz. Evidence
for absence of latch-bridge formation in muscular saphenous arteries.
Am J Physiol Heart Circ Physiol 291: H138–H146, 2006. First
published February 3, 2006; doi:10.1152/ajpheart.00977.2005.—
Large-diameter elastic arteries can produce strong contractions indef-
initely at a high-energy economy by the formation of latch bridges.
Whether downstream blood vessels also use latch bridges remains
unknown. The zero-pressure medial thickness and lumen diameter of
rabbit saphenous artery (SA), a muscular branch of the elastic femoral
artery (FA), were, respectively, approximately twofold and half-fold
that of the FA. In isolated FA and SA rings, KCl rapidly (<16 s)
caused strong increases in isometric stress (1.2 × 10⁵ N/m²) and
intracellular Ca²⁺ concentration ([Ca²⁺]ᵢ; 250 nM). By 10 min,
[Ca²⁺]ᵢ declined to ~175 nM in both tissues, but stress was sustained
in FA (1.3 × 10⁵ N/m²) and reduced by 40% in SA (0.8 × 10⁵ N/m²).
Reduced tonic stress correlated with reduced myosin light chain
(MLC) phosphorylation in SA (28 vs. 42% in FA), and simulations
with the use of the four-state kinetic latch-bridge model supported the
hypothesis that latch-bridge formation in FA, but not SA, permitted
maintenance of high stress values at steady state. SA expressed more
MLC phosphatase than FA, and permeabilized SA relaxed more
rapidly than FA, suggesting that MLC phosphatase activity was
greater in SA than in FA. The ratio of fast-to-slow myosin isoforms
was greater for SA than FA, and on quick release, SA redeveloped
isometric force faster than FA. These data support the hypothesis that
maintained isometric force was 40% less in SA than in FA because
expressed motor proteins in SA do not support latch-bridge formation.

vascular smooth muscle; myosin light chain phosphorylation; KCl;
myosin isoforms; calcium

ISOLATED LARGE ELASTIC ARTERIES can maintain high levels of
stimulus-activated isometric stress with a high-energy econ-
omy (5, 31, 49). Myosin (M) hydrolyzes ATP before entry into
an actomyosin attachment-force generation-detachment cycle,
and active stress is proportional to the numbers of attached
actomyosin cross bridges. Myosin light chain (MLC) phos-
phorylation (1, 4, 18) permits actomyosin strong binding and
entry into the cross-bridge cycle (42) by accelerating phosphate
release from the head of myosin heavy chain (MHC) (12, 41).
A consequence of this thick filament-regulated activation
mechanism is that MLCs theoretically may be dephosphory-
lated when cross bridges are detached [actin (A) + phosphor-
ylated myosin (Mp) → A + M] or attached (AMp → AM).
The motor protein is "turned off" by the former, whereas the
latter, at least in the vascular smooth muscle (VSM) of elastic

arteries, is proposed to cause formation of a cross bridge with
a very slow rate of detachment, termed a latch bridge (AM)
(14, 15) (see Fig. 1). Importantly, early studies revealed a
surprising finding that maximum stress may be maintained in
VSM of elastic arteries at very low levels of MLC phosphor-
ylation (5).

One of the most highly studied models of smooth muscle
contraction is the Hai-Murphy four-state kinetic model (15),
which quantified and explained the concept proposed earlier
(5) that, to maintain higher levels of stress despite lower levels
of phosphorylated (i.e., actively cycling) cross bridges (AMp),
a second cross-bridge type (latch bridge, AM) must participate.
In this model, phosphorylated cross bridges perform the dual
role of developing and maintaining active force, whereas
attached cross bridges that become dephosphorylated while in
the attached state become latch bridges that function primarily,
if not solely, to maintain force (i.e., they cycle slowly or not at
all and therefore do not contribute to force development).
However, by prolonging the average value for the motor
protein duty cycle (6), latch bridges are proposed to introduce
an internal load against which cycling cross bridges act, result-
ing in a reduction in net cross-bridge cycling rates. In intact
elastic arteries, the maximum velocity of muscle shortening, a
measure of the rate of cross-bridge cycling, is indeed a regu-
lated parameter that correlates with the level of MLC phos-
phorylation (7, 33). However, modulation of cross-bridge cy-
cling rates have also been attributed to other events related to
a reduction in intracellular Ca²⁺ concentration ([Ca²⁺]ᵢ) (44).

The Hai-Murphy four-state kinetic model is robust enough
to have successfully predicted principal mechanical behaviors
of vascular (14, 15, 33, 39), airway (24, 50), molluscan (3, 50),
and *Aplysia* (50) smooth muscles. Most recently, a modified
latch-bridge model has been formulated that can successfully
predict the additional contribution of thin-filament regulation
to control of smooth muscle contraction (16). It is now clear
that large elastic arteries and other tonic smooth muscles utilize
a latch-bridge or catchlike mechanism to regulate the sustained
phase of force maintenance [see reviews by Murphy (27) and
Somlyo et al. (45)] and that phasic smooth muscles that do not
normally function to maintain high levels of stress for pro-
longed periods may not [see review by Somlyo et al. (45)].

The arterial side of the vascular tree is a complex organ
system composed of large-diameter elastic arteries, smaller
diameter and more muscular distributing arteries, and much
smaller feed arteries and arterioles (40). What remains to be
determined is whether all artery "types" behave biochemically
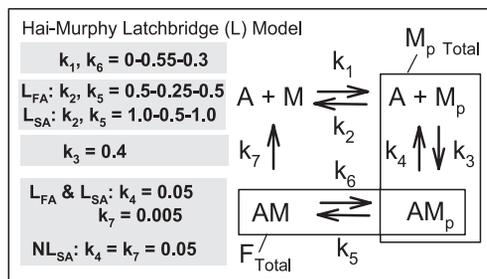
 http://www.ajpheart.org

Fig. 1. Hai-Murphy 4-state kinetic latch-bridge (L) model used for simulations displayed in Figs. 6 and 7. A, actin; M, myosin; Mp, myosin light chain (MLC)-phosphorylated species where myosin is in unattached state; AMp, MLC-phosphorylated species where myosin is in actin-attached (cross bridge) state; AM, dephosphorylated, attached cross bridges that can bear a load but that do not contribute to force development (latch bridges). Total force (F) = AM + AMp. Total MLC phosphorylation = Mp + AMp. L_{FA} and L_{SA}, model simulations where $K_7 = 0.1$-fold K_4 (latch bridge is included) for, respectively, femoral artery (FA) and saphenous artery (SA). NL_{SA}, model simulation where a latch bridge is absent [$K_7 = K_4$; i.e., no latch bridge (NL)].

and mechanically like large elastic arteries and utilize a latch-bridge mechanism to control tonic force maintenance. For this reason, the Hai-Murphy four-state kinetic model was used in the present study to determine whether tonic force maintenance of the muscular saphenous artery (SA), a major branch of the elastic femoral artery (FA), can be explained by latch-bridge formation. By studying FA and SA, we were able to use arterial smooth muscles from the same peripheral vascular bed to directly identify and compare underlying mechanisms controlling tonic arterial contractile behavior in two different artery types. Biochemical evidence also was obtained to support or reject the hypothesis that latch-bridge formation is a requirement for force maintenance in muscular arteries as it is in elastic arteries. In particular, time-dependent changes in isometric force, [Ca^{2+}]$_i$, and MLC phosphorylation were measured and compared in SA and FA. In addition, rates of force redevelopment, an estimate of cross-bridge cycling rates (6), were compared in SA and FA. Finally, expression levels of MHC and 17-kDa MLC isoforms and additional major proteins that participate in the contractile process (i.e., the general contractile proteome) of SA and FA were compared with each other and to detrusor and stomach antrum, classically phasic visceral smooth muscles that, unlike elastic artery, do not develop latch [see review by Somlyo et al. (45)].

METHODS

Tissue preparation, artery diameter, and isomeric force. All experiments involving animals were conducted within the appropriate animal welfare regulations and guidelines and were approved by the Virginia Commonwealth University Institutional Animal Care and Use Committee. Smooth muscle tissues from female New Zealand white rabbits (3–4 kg) were prepared as previously described (34) and stored in cold (4°C) physiological saline solution [PSS; in mM: 140 NaCl, 4.7 KCl, 1.2 MgSO₄, 1.6 CaCl₂, 1.2 NaHPO₄, 2.0 MOPS adjusted to pH 7.4, 0.02 Na₂ethylenediamine tetraacetic acid to chelate heavy metals, and 5.6 D-glucose made with high-purity (17 MΩ) deionized water]. The endothelium of tissues cleaned by microdissection (Olympus SZX12) was removed by gently rubbing the intimal surface with a metal rod. Arteries were cut into 2- to 3-mm-wide rings for most studies. Thin longitudinal detrusor strips free of underlying urothelium and overlying serosa were dissected from bladders. Contractile force (F) was measured as previously described

(34) using a Myograph System-610M (Danish Myo Technology). The optimum muscle length (L_o) for which active force was maximum was determined for each tissue by using an abbreviated length-tension curve and PSS in which 110 mM KCl was substituted iso-osmotically for NaCl (KPSS) as the stimulus (17, 32). To eliminate effects of norepinephrine and acetylcholine released from nerves, 1 μM phentolamine and atropine were used to block, respectively, α_1-adrenergic and muscarinic receptors in arteries and detrusor. Muscle stress (S) in N/m² was calculated as follows: [F (in g) × 9.807 × 10^{-3} N/g]/{[wet wt (in mg)/L_o (in mm)] × 9.52×10^{-7} m²·mm/mg}.

Tissue histology. To measure medial wall thickness and numbers of cell layers in the media, arterial rings were fixed (glutaraldehyde), embedded (PolyBed 812 resin), and sectioned with an ultramicrotome, transferred to a microscope slide, and stained with 0.1% Toluidine blue/0.1% methylene blue/0.1% azure II in 1% sodium borate solution (22). Wall thickness of each artery was measured, and the numbers of cell layers for each cross section were counted with a microscope (Olympus IX71) and OpenLab software (Improvision).

Polyacrylamide gel electrophoresis. Two-dimensional (isoelectric focusing/SDS) PAGE was performed as previously described (34, 47) to measure the degree of MLC phosphorylation and the fractional expression of the 17-kDa MLC isoforms MLC$_{17a}$ and MLC$_{17b}$. Expression levels of MLC phosphatase catalytic subunit (PP1δ), MLC phosphatase large molecular weight regulatory targeting subunit (MYPT-1), and RhoA kinase α (ROKα) were measured by SDS-PAGE and Western blot analysis as described previously (35). Protein loading was verified to be constant across all lanes by MEMCode (Pierce) staining. Dilutions of primary antibodies were 1:500 for anti-PP1δ (Upstate) and anti-MYPT-1 (BD Transduction) and 1:200 for anti-ROKα (Santa Cruz Biotechnology). Horseradish peroxidase-conjugated goat polyclonal antibody was used as secondary antibody, and the amounts of specific protein were detected by enhanced chemiluminescence (Amersham) and quantified after digitization by Scion Image Software. For MHC isoform expression analyses, rabbit tissues were homogenized in 0.125 M Tris, 2% SDS (wt/vol), 20% glycerol, 0.1% bromophenol blue (wt/vol), and 20 mM dithiothreitol. MHCs were resolved on low cross-linking SDS gels (11), and immunoblotting was performed as previously described (8). Polyclonal antibodies to the SMB (plus seven-amino acid head insert isoform) and SMA (minus seven-amino acid head insert) smooth muscle MHC isoforms were generated in rabbits by using the following peptides (SMA polypeptide - ′N′–KKDTSITGELEC–′C′; SMB polypeptide-′N′– QGPSLAYGELEC–′C′). Antiserum was tested on ELISA against expressed SMA and SMB subfragment 1 polypeptides. Both antibodies were shown to have at least 100-fold higher affinity for their appropriate antigen than for the alternative isoforms. Smooth muscle and nonmuscle MHC-specific antisera were obtained from Biomedical Technologies (Stoughton, MA). Western immunoblots were reacted as reported previously (10).

[Ca^{2+}]$_i$. [Ca^{2+}]$_i$ was measured as previously described (34). Tissues at L_o in an aerated muscle chamber designed for microscopic imaging (Danish Myo Technology) were placed on the stage of an inverted microscope (Olympus IX71) and loaded for 2.5 h with 7.5 μM fura 2-PE3 (AM) and 0.01% (wt/vol) Pluronic F-127 (TefLabs, Austin, TX) to enhance solubility. Fluorescence emission at 510 nm was collected by a photomultiplier tube for excitations at 340 and 380 nm (DeltaRam V, Photon Technologies, Lawrenceville, NJ), and emission intensities were expressed as 340/380 nm ratios with the use of Felix software (Photon Technology International) to measure changes in [Ca^{2+}]$_i$. Minimum and maximum fluorescence ratios were obtained by treating tissues with, respectively, a Ca^{2+}-free KPSS containing 5 mM EGTA and 30 μM ionomycin and a high-calcium (3.2 mM Ca^{2+}) KPSS containing 30 μM ionomycin. Background fluorescence, determined by incubating tissues in 4 mM MnCl₂ plus 30 μM ionomycin, was subtracted from all 340 and 380 nm signals before calculation of the 340/380 nm fluorescence ratios. [Ca^{2+}]$_i$ was calculated as described previously (13).

Tissue permeabilization. Artery rings at L_o were depleted of sarcoplasmic reticular Ca^{2+} by contracting three times with 10 μM phenylephrine in a Ca^{2+}-free solution. Tissues were then permeabilized at 5°C for 45 min with β-escin (40 μM for FA and 100 μM for SA; the higher concentration for SA was used because of its thicker media), and permeabilization continued for 60 min at 30°C. The initial treatment with β-escin at a low temperature helps the slow penetration and/or binding of β-escin to the surface membrane of the smooth muscle cells (23). β-Escin was dissolved in a "relaxing solution" containing 74.1 mM potassium methanesulfonate, 4.0 mM magnesium methanesulfonate, 4 mM Na_2ATP, 4 mM EGTA, 5 mM creatine phosphate, and 30 mM PIPES and neutralized with 1 M KOH to pH 7.1 at 20°C. Ionic strength was kept constant at 0.18 M by adjusting the concentration of potassium methanesulfonate. To activate muscle contraction at Ca^{2+}-clamped levels of 1 μM (pCa = 6) free Ca^{2+}, a "contracting solution" was made by including the appropriate volume of a 1 M $CaCl_2$ stock (Fluka Chemicals) as determined by using WEBMAXC (30). Calmodulin (1 μM) was added to the solutions throughout each experiment to compensate for its loss during permeabilization. To induce relaxation for relaxation velocity measurements, tissues precontracted by pCa = 6 contracting solution were rapidly washed in the relaxing solution (pCa = 9) containing 3 μM wortmannin to inhibit MLC kinase activity.

Latch-bridge model simulation. The Hai-Murphy kinetic four-state latch-bridge model (Fig. 1) was simulated with the use of Matlab 6.5 with Simulink 5.0 (MathWorks) by using the same initial conditions and assumptions as those used by Hai and Murphy (15). Because Matlab 6.5 permits the use of time-varying constants, this feature was employed for rate constants simulating changes in MLC kinase and phosphatase activities to more closely reflect the time-varying changes in $[Ca^{2+}]_i$ (and, thus, MLC kinase activity) and regulation of MLC phosphatase by ROK [see review by Ratz et al. (37)]. We used modeling rate constants (in s^{-1}) that were very similar to those used by Hai and Murphy to predict the behavior of the tonic swine carotid artery (15). However, rather than stepping K_1 and K_6 values from 0 to 0.55 for 5 s and then down to 0.30 for the remainder of the simulated stimulation period to mimic changes in MLC kinase activity due to changes in $[Ca^{2+}]_i$ (15), we used similar values but modeled a more gradual change to more closely follow the change in $[Ca^{2+}]_i$ measured in SA and FA (see Fig. 6, *C* and *D*). We also modeled a small temporal change in K_2 and K_5 values to reflect recent data (37) indicating that KCl can activate ROK and produce a transient small increase in MYPT-1 phosphorylation that may transiently reduce MLC phosphatase activity (see Fig. 6, *E* and *F*).

Drugs. Wortmannin, Y-27632, and ionomycin were from Calbiochem (La Jolla, CA), and all other drugs were from Sigma (St. Louis, MO). β-Escin was dissolved in DMSO for a stock concentration of 10 mM. Ionomycin was dissolved in 100% ethanol for stock solutions of 10 mM. Vehicles (DMSO and ethanol) were added to control tissues at no more than 0.1%, which had no effect on contractions. All other drugs were dissolved in distilled water.

Statistics. The null hypothesis was examined with the use of Student's *t*-test (when 2 groups were compared) or a one-way ANOVA. To determine differences between groups following ANOVA, the Student-Newman-Keuls post hoc test was used. In all cases, the null hypothesis was rejected at $P < 0.05$. For each study described, the *n* value was equal to the number of rabbits from which arteries were taken. Statistical analyses and curve fitting were performed with the use of Prism 3.02 (GraphPad Software, San Diego, CA).

RESULTS

Structure. Of the two major branch arteries that bifurcate from the femoral artery (FA) just cranial to the knee, only the deep femoral (DF) artery grossly (Fig. 2*Aa*) and histologically (Fig. 2, *Ab–Ad*) represented an extension of the FA, whereas
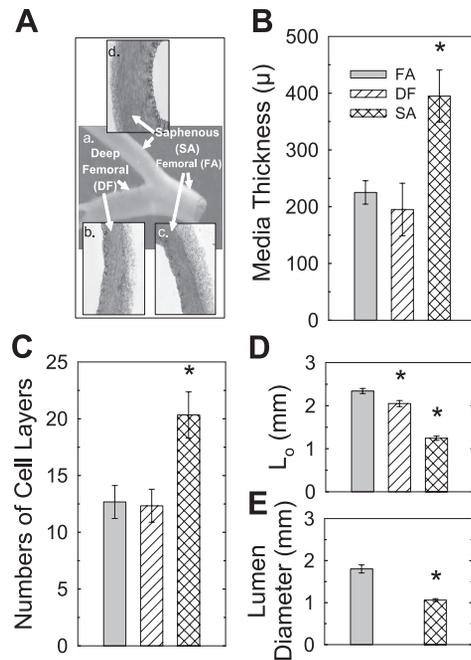

Fig. 2. Gross (*Aa*) and fine (*Ab–Ad*) structures of rabbit FA (*Aa* and *Ac*), deep femoral (DF; *Aa* and *Ab*), and SA (*Aa* and *Ad*) arteries. SA and DF are downstream branches that bifurcate from FA. Medial wall thickness (*B*) and numbers of cell layers within media (*C*) of FA and DF were identical. Optimum length (L_o) for muscle contraction (*D*), a muscle mechanical measurement that reflects lumen diameter (*E*), of DF was slightly shorter than FA L_o. SA was approximately twofold thicker (*B*) because of approximately twofold more medial cell layers (*C*) but displayed a shorter L_o (*D*) correlating with a smaller lumen diameter (*E*) than the FA. Data in *B–E* are means ± SE and *n* = 3, except for *D*, where *n* = 13, and *E*, where *n* = 4 (FA) and 9 (SA). *$P < 0.05$ compared with FA.

the SA was structurally different from the FA. For example, the FA and DF artery had equivalent medial thicknesses (Fig. 2*B*) and numbers of cell layers within the media (Fig. 2*C*) and nearly equivalent L_o for muscle contraction (Fig. 2*D*), a muscle mechanical measurement that reflects artery lumen diameter. However, compared with FA, SA media were approximately twofold thicker (Fig. 2*B*) because of approximately twofold more medial cell layers (Fig. 2*C*) but displayed a shorter L_o by approximately one-half (Fig. 2*D*), correlating with a smaller zero-load lumen diameter (Fig. 2*E*).

Stress, $[Ca^{2+}]_i$, and MLC phosphorylation. KCl produced tonic contractions in the FA (Figs. 3, *A* and *B*) and DF artery (Fig. 3*B*) with equivalent time-dependent force values. By contrast, SA produced a biphasic contraction in response to stimulation with KCl consisting of an early peak increase in stress equal to the maximum tonic stress produced by FA followed by a decline from the peak value by 5 and 10 min to a value ~60% that produced by FA (Fig. 3*A*; $P < 0.05$). A maximum phenylephrine concentration (10 μM), like KCl, also produced tonic and biphasic contractions in, respectively, FA and SA (data not shown). Despite divergent temporal changes in stress, FA and SA produced equivalent temporal changes in $[Ca^{2+}]_i$ when stimulated with KCl (Fig. 3, *C* and *D*). Thus the difference in steady-state stress between FA and SA could not be ascribed to a difference in $[Ca^{2+}]_i$.

KCl produced a rapid increase in the degree of MLC phosphorylation from a basal value of ~5–40% within 4 s in both FA and SA (Fig. 3*E*). However, MLC phosphorylation
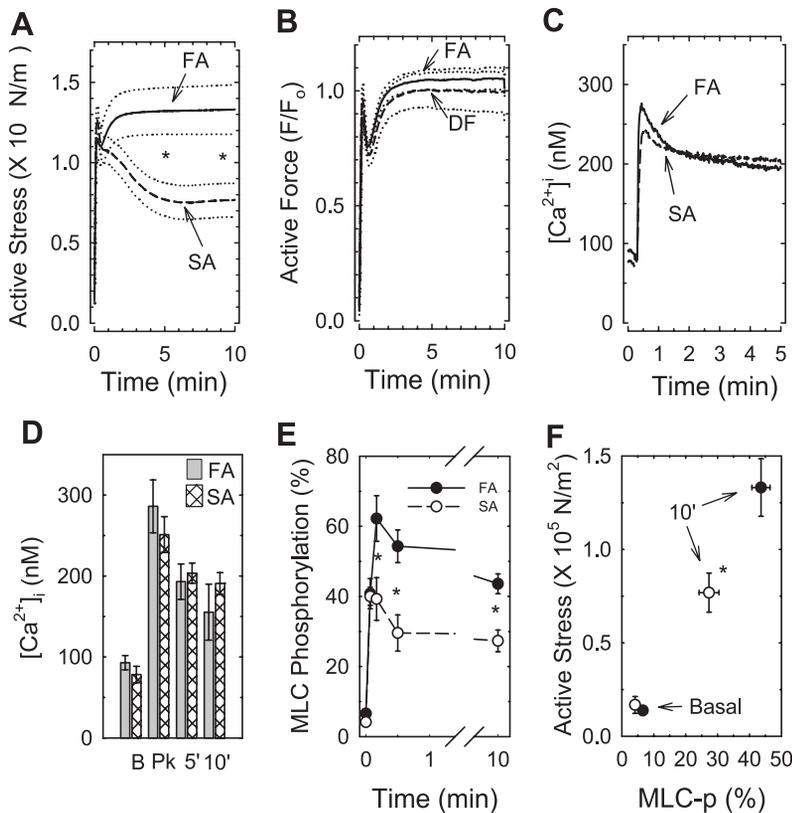
Fig. 3. FA and SA produced equivalent early (16.2 ± 1.2 s) peak increases in stress on stimulation with KCl (~1.2 × 10⁵ N/m²) that remained at high levels for at least 10 min in FA but declined by 5 min in SA to ~0.8 × 10⁵ N/m² (*A*). DF artery produced a temporal contractile (KCl) profile identical to that produced by FA (*B*). Despite different contractile profiles, FA and SA produced an identical time-dependent, KCl-induced profile in intracellular Ca²⁺ concentration ([Ca²⁺]ᵢ; *C* and *D*). B and Pk, basal and peak, respectively (*D*). From 10 s (*E*) to 10 min (*E* and *F*), KCl produced greater increases above basal level in MLC phosphorylation (MLC-p) in FA than in SA. Data are means (solid and dashed lines in *A*–*C*, symbols in *E* and *F*, and bars in *D*) ± SE (dotted lines in *A* and *B*). For clarity, SE values were removed from curves in *C* and included in *D*; n = 4–10. *P < 0.05 compared with FA.

continued to increase to over 60% by 10 s in FA but remained at ~40% in SA, a value statistically lower than that produced by FA (Fig. 3*E*). MLC phosphorylation declined in both FA and SA to lower steady-state values. However, SA reached a steady-state MLC phosphorylation value of ~28% within 30 s and remained at that level for at least 10 min, whereas FA produced a more gradual decline to a steady-state value of ~42% at 10 min (Fig. 3, *E* and *F*). The correlation in MLC phosphorylation and stress values (Fig. 3*F*) suggests that the biphasic nature of the KCl-induced contraction produced by SA (in which the level of tonic force was less than that produced by FA) was caused by the reduced level of steady-state MLC phosphorylation in SA compared with FA.

Estimate of MLC phosphatase activity and expression of MLC phosphatase. The rate of relaxation of permeabilized arterial smooth muscle is limited by the rate of MLC phosphatase activity (25). Thus the rate of relaxation from a precontracted state induced by exposure of permeabilized tissues to a Ca²⁺-free solution containing a MLC kinase inhibitor can be used as an indirect measure of the MLC phosphatase activity in Ca²⁺-clamped but otherwise intact smooth muscle tissue (21). Our data showed that SA produced a much more rapid relaxation compared with FA when tissues precontracted at pCa = 6 were exposed to a relaxing solution (containing EGTA; see METHODS) and the MLC kinase inhibitor wortmannin (Fig. 4*A*). The half-time for relaxation was nearly 2 min in FA but was <1 min in SA (inset, Fig. 4*A*). To ensure that relaxation rates reflected rates of MLC dephosphorylation in both FA and SA, MLC phosphorylation and force were measured simultaneously in one set of tissues. The nearly linear relationship between MLC phosphorylation and force (see *inset*, Fig. 4*B*) supports the conclusion that relaxation rates in permeabilized

tissues can be a surrogate measure of MLC dephosphorylation and reflect MLC phosphatase activity (21, 25). These data suggest that the lower MLC phosphorylation levels produced in intact (not permeabilized) SA compared with FA during a KCl-induced contraction are caused by a higher intrinsic MLC phosphatase activity in SA compared with FA.

We compared, in FA and SA, expressed levels of MLC phosphatase catalytic (PP1δ) and large regulatory (MYPT-1) subunits, and ROKα, an enzyme that plays a key role in the regulation of MLC phosphatase activity in KCl-induced tonic contractions [see review by Ratz et al. (37)]. SA expressed nearly twofold more PP1δ and ~1.3-fold more MYPT-1 than did FA, but both arteries expressed equal levels of ROKα (Fig. 4, *C* and *D*). These data suggest that one possible cause for increased MLC phosphatase activity in SA compared with FA is that SA expresses more MLC phosphatase such that the overall MLC phosphatase-to-kinase activity ratio is higher in SA.

Effects of wortmannin and Y-27632. To determine whether MLC kinase and ROK-dependent MLC phosphatase play similar or different roles in SA and FA, intact tissues were contracted in the presence of the MLC kinase inhibitor wortmannin and the ROK inhibitor Y-27632. Wortmannin produced identical inhibitions of both peak (Fig. 5*A*) and steady-state (Fig. 5*B*) contractions in SA and FA. Y-27632 likewise inhibited steady-state contractions in SA and FA with equal potency (Fig. 5*D*) and had no effect on the peak contractile response produced by SA and FA (Fig. 5*C*). In support of the previous finding from our laboratory (36), Y-27632 inhibited both peak and steady-state contractions of a visceral smooth muscle (detrusor; Fig. 5, *C* and *D*). These data suggest that additional regulatory systems other than MLC kinase and ROK-dependent MLC phosphatase are not required to explain
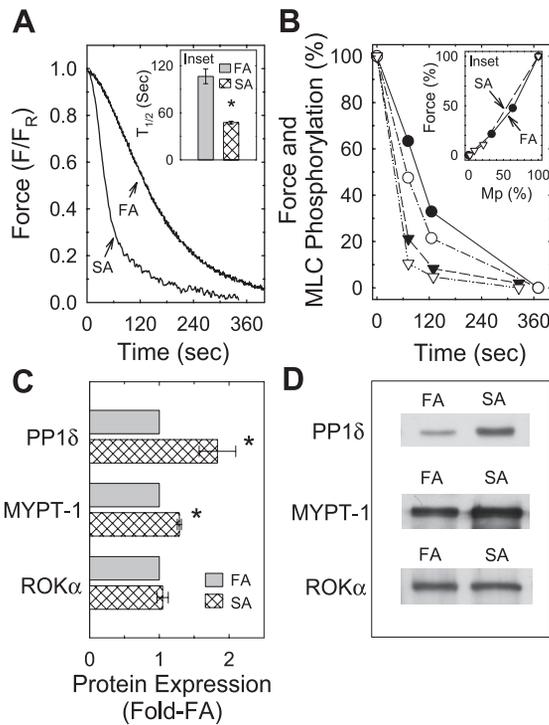
Fig. 4. Time-dependent relaxation [*A*; *inset*: half-time ($t_{1/2}$) for relaxation] and reduction in MLC phosphorylation [*B*; *inset*: relationship between force and MLC phosphorylation (Mp)] produced during relaxation in β-escin-permeabilized rings of FA and SA. Force tracings in *A* are examples. Data in *A*, *inset* are means ± SE ($n = 4$); *$P < 0.05$ compared with FA; data in *B* (FA, circles; SA, inverted triangle; %force, closed symbols; %Mp, open symbols) are from one artery ($n = 1$). Average values (*C*) and Western blot examples (*D*) of comparisons of expression of catalytic subunit of protein phosphatase (PP1δ; MLC phosphatase is a PP1δ subtype), myosin phosphatase targeting subunit (MYPT-1), and RhoA kinase α (ROKα, a regulator of MLC phosphatase) in FA and SA. Gel lanes were loaded with 20 μg (for PP1δ), 10 μg (for MYPT-1), and 50 μg (for ROKα) protein. Data for SA are means ± SE ($n = 6$); *$P < 0.05$ compared with FA.

KCl-induced steady-state (tonic phase) contractions of SA and FA.

Latch-bridge model. The Hai-Murphy four-state kinetic latch-bridge model (see Fig. 1) was employed to determine whether the reduction in KCl-induced steady-state MLC phosphorylation in SA compared with FA was sufficient to explain the biphasic contractile behavior of SA. With a K_4 value of 0.05, a K_3 value of 0.4, and, as in the original Hai-Murphy model (15), a K_7 (latch bridge) value one-tenth that of the K_4 value ($K_7 = 0.005$), the modeled temporal change in MLC phosphorylation fit closely the empirically derived MLC phosphorylation data for FA (Fig. 6*G*). Our data showing that steady-state MLC phosphorylation (see Fig. 3, *E* and *F*), but not [Ca^{2+}]$_i$ (see Fig. 3, *C* and *D*), was less in SA than FA suggested that MLC phosphatase in SA was greater than that in FA. Thus K_2 and K_5 values used to model FA behavior were doubled to model SA behavior (Fig. 6*F*). The resulting modeled change in MLC phosphorylation fairly closely matched the empirical MLC phosphorylation data for SA (Fig. 6*H*).

The force response predicted on the basis of a latch-bridge-to-phosphorylated cross-bridge detachment ratio (K_7/K_4) of 0.1 very closely matched our empirical data for FA (Fig. 6*A*, model L$_{FA}$) but was a poor match for SA (Fig. 6*B*, model L$_{SA}$). When the detachment rate for a latch bridge

was made to equal the detachment rate for a phosphorylated cross bridge (i.e., $K_7/K_4 = 1$), the modeled force profile more closely fit the actual empirical data for SA (Fig. 6*B*, model NL$_{SA}$).

Because of the steeply hyperbolic dependency of steady-state force on steady-state MLC phosphorylation in elastic arteries such as the carotid artery, where force "saturates" at modest levels of MLC phosphorylation (33, 34), a reduction in MLC phosphorylation from over 40% to just under 30% will not necessarily result in a significant reduction in force. Rather, total force will remain relatively constant as the fraction of phosphorylated, attached cross bridges (AMp) is reduced and the fraction of unphosphorylated, attached cross bridges (AM, latch bridges) is proportionally increased. That is, the latch bridge-modeled force profiles for FA (Fig. 7*A*, AMp + AM, dashed line) and SA (Fig. 7*A*, AMp + AM, solid line) were found to be nearly equivalent despite large differences in MLC phosphorylation values because the proportion of cross bridges contributing to steady-state (5 min) force for the FA was ~60% latch bridge (Fig. 7*A*, AM, dashed line) and ~40% phosphorylated, attached, cycling cross bridge (Fig. 7*A*, AMp, dashed line), whereas that for SA was ~73% latch bridge (Fig. 7*A*, AM, solid line) and ~27% phosphorylated, attached, cycling cross bridge (Fig. 7*A*, AMp, solid line). Thus the reason why a reduction in the level of MLC phosphorylation from ~42% to ~28% did not result in a comparable reduction in force in the four-state kinetic simulation has a straightforward and readily predictable explanation based on the Hai-Murphy latch-bridge model.

Elimination of the latch bridge (without eliminating the myosin species, AM) by making K_4 equal K_7 (no latch; NL$_{SA}$, Fig. 7*B*; see also Fig. 1) caused force to fall temporally with the fall in MLC phosphorylation (i.e., force became biphasic, Fig.
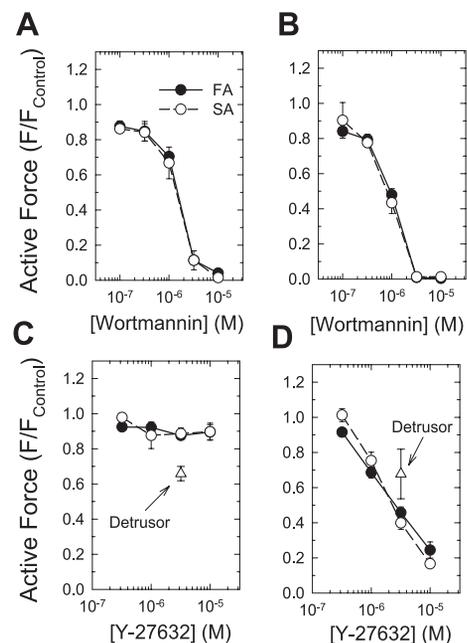

Fig. 5. Effect of wortmannin (MLC kinase inhibitor) and Y-27632 (ROK inhibitor) on KCl-induced early peak (*A* and *C*) and tonic (10 min; *B* and *D*) force in FA and SA. For comparison, effect of Y-27632 on bladder wall [detrusor (Det)] smooth muscle was included (triangles; *C* and *D*). Data are means ± SE ($n = 3-5$).
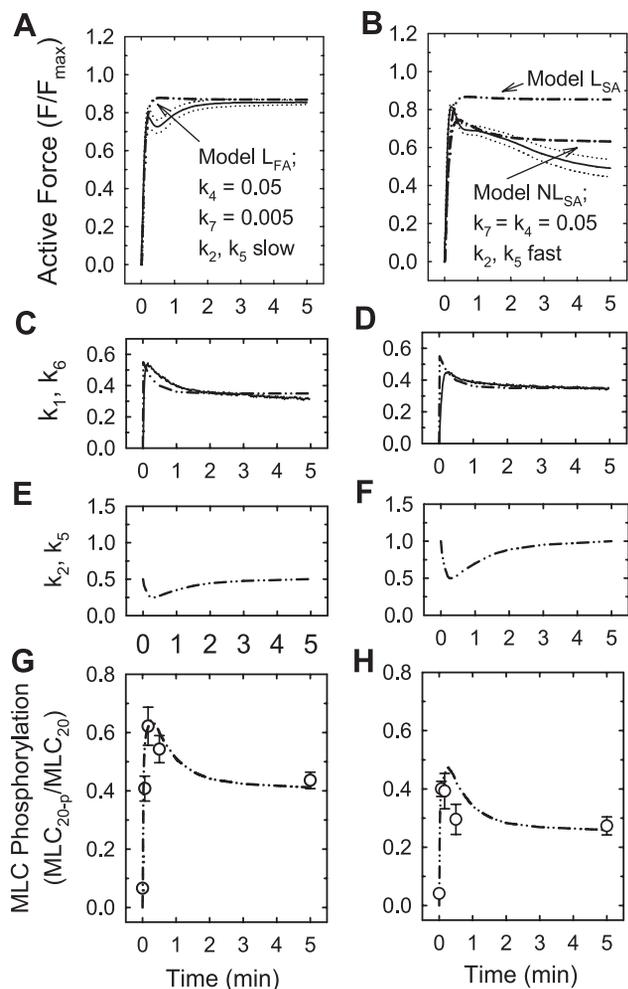
Fig. 6. Hai-Murphy 4-state kinetic latch-bridge model simulation (dash-dotted lines) and empirical data (solid lines and open symbols, average values; dotted lines, SE) for FA and SA. L_{FA} (*A*) and L_{SA} (*B*) are simulated contractile profiles, where $K_7 = 0.1$-fold K_4 (i.e., K_7 refers to very slow detachment rate of a latch bridge, AM → A + M compared with a cross bridge, AMp → A + Mp; see Fig. 1) for, respectively, FA and SA. NL_{SA} (*B*) is a simulated contractile profile for SA, where $K_7 = K_4 = 0.05$ (i.e., a latch-bridge state is absent because rates of detachment of AM and AMp are equivalent). Empirical data for *C* and *D* are normalized Ca^{2+} tracings derived from Fig. 3*C*. Empirical MLC phosphorylation data are from Fig 3*E*.
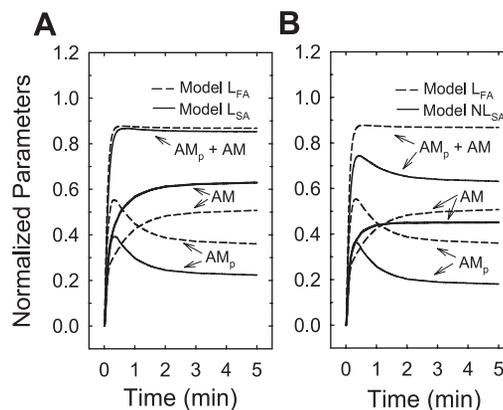

Fig. 7. Hai-Murphy 4-state kinetic latch-bridge model simulations for FA and SA comparing time-dependent changes in total force (AMp + AM) and two force-producing species (attached, phosphorylated cross bridges, AMp, and attached, unphosphorylated cross bridges, AM). When compared with the relatively low level of latch-bridge species formed (*A*, dashed line, AM) at a relatively high level of simulated MLC phosphorylation (*A*, dashed line, AMp) mimicking empirical data from FA, a lower level of simulated MLC phosphorylation (*A*, solid line, AMp) that mimics level found to occur in SA yields a higher simulated level of latch-bridge species (*A*, solid line, AM). Thus, despite a lower level of MLC phosphorylation in SA, latch-bridge formation would disallow a temporal fall in tonic force, i.e., biphasic contractile behavior seen empirically in SA (AMp + AM = force). Absence of latch-bridge state (*B*, NL_{SA}, $K_7 = K_4$) in simulation permits a temporal fall in force, resulting in a more biphasic contraction (*B*, solid line compared with dashed line, AMp + AM) that more closely mimics empirical temporal force profile produced in SA on KCl-induced stimulation.

latch bridges, then SA should recontract more slowly than FA on quick release at ~10 min of contraction because SA produced significantly lower MLC phosphorylation levels at this time (see Fig. 3, *E* and *F*). Our empirical data revealed the opposite, namely, that the rate of force redevelopment produced by SA was significantly higher than that for FA (Fig. 8). With the use of a curve-fitting program (GraphPad Prism), the rate of force redevelopment for both arteries produced a good

7*B*, AMp + AM, solid line) because of a reduction in the amount of latch bridges contributing to force [Fig. 7*B*; compare AM, solid line (SA) to AM dashed line (FA)]. These data support a model for contraction of the muscular SA in which there is an absence of latch bridges.

Rates of force redevelopment on quick release. Steady-state levels of MLC phosphorylation correlate with steady-state levels of the velocity of muscle shortening (33), and the rate of force redevelopment on quick release (Fig. 8*A*) is a measure of the velocity of muscle shortening (6). The proposed reason for a correlation between MLC phosphorylation levels and the rate of force redevelopment is that the ratio of cycling cross bridges to latch bridges (AMp/AM) is higher at higher levels of MLC phosphorylation (Fig. 5 in Ref. 15; see also Fig. 7*A* for an example). Latch bridges are proposed to introduce an internal load against which cycling cross bridges operate, causing slowing of the rate of muscle shortening. Thus, if SA contains

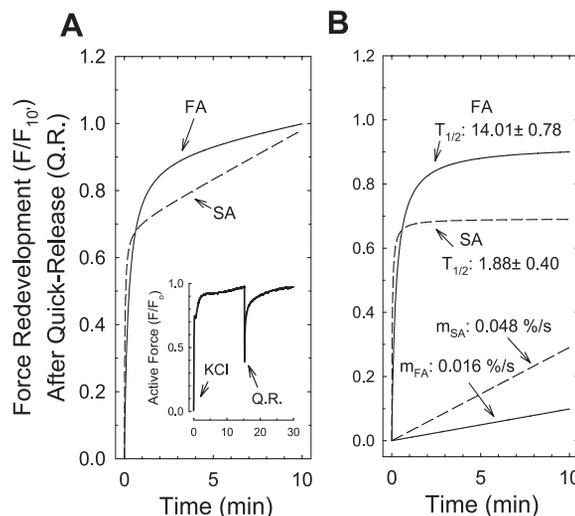Fig. 8. *A*: hyperbolic + linear curve provides a good modeling fit ($r^2 > 0.97$) for force redevelopment after quick, 10% step decrease in muscle length (*inset*; QR, quick release) during steady state of KCl-induced contraction for both FA and SA. *B*: half-lives ($t_{1/2}$) of hyperbolic component and slopes (m) of linear component of curves for FA and SA and individual hyperbolic and linear curve; $n = 4$.

fit ($r^2 = 0.996$ for FA; $r^2 = 0.974$ for SA) to an equation consisting of one fast hyperbolic and one slower linear component (Fig. 8A). The half-time for force redevelopment for the hyperbolic component of FA was over sevenfold longer than that for SA (i.e., the rate of force redevelopment for SA was over sevenfold faster than FA; Fig. 8B), and the slope of the slower, linear component for SA was threefold faster than for FA (m_{SA} and m_{FA} in Fig. 8B). These data together support the hypothesis that FA does, but SA does not, form latch bridges to maintain steady-state force.

Smooth muscle motor protein expression levels. Higher rates of force redevelopment for SA compared with FA support the hypothesis that SA contains "faster" motor protein isoforms than FA [see Arner et al. (2) for a review]. To test this hypothesis, the relative expression of MLC_{17a} and MLC_{17b} were examined using two-dimensional PAGE, and smooth muscle MHC isoforms that do (SMB) and do not (SMA) contain a seven-amino acid insert were examined by using Western blot analysis and selective antibodies. The FA, DF artery, and tonic renal artery (RA) displayed ~50–60% MLC_{17a}, whereas SA and a classically phasic visceral smooth muscle (detrusor) displayed 90–100% MLC_{17a} (Fig. 9A). The tonic arteries, aorta, carotid artery, FA and RA, and a visceral smooth muscle known to produce sustained, tonic contraction, the stomach fundus, displayed higher relative expression levels of SMA compared with SMB, whereas SA and a phasic visceral smooth muscle (known to contract only transiently and not maintain high tonic force levels), the stomach antrum, displayed higher relative levels of SMB compared with SMA (Fig. 9, *Bd* and *Be*). None of the smooth muscles examined expressed enough nonmuscle myosin to be detected when compared with an equal protein loading of platelets that express nonmuscle rather than smooth muscle myosin (Fig. 9Bc). These data support the notion that SA produced faster force redevelopment than FA despite lower MLC phosphorylation levels at steady state because SA expressed quantitatively more of the "faster" (SMB and MLC_{17a}) compared with "slower" (SMA and MLC_{17b}) myosin isoforms (2).

Selective proteomic analysis. On the basis of its temporal contractile profile, rate of force redevelopment, and motor protein isoform composition, the SA may be categorized along with visceral smooth muscles represented by detrusor and stomach antrum as a "phasic" smooth muscle because these muscles produce "fast" contractions and do not produce strong, sustained force during the tonic phase of contraction. Thus the contractile phenotype and the motor protein expression of SA are more similar to that of most visceral smooth muscles than to its "parent" elastic arterial smooth muscle, the FA. Regulation of smooth muscle contraction requires the interaction of many complex signaling, metabolic, and structural systems, and whether some arterial muscles are more closely related overall to visceral smooth muscles or to each other is an important question that remains to be determined. To examine whether the general protein expression profile of SA is more like that of a phasic visceral smooth muscle or a tonic arterial smooth muscle, an initial proteomic analysis was performed.

The abundance of highly expressed proteins relative to actin in FA, SA, and detrusor were compared by using one-dimensional PAGE (Fig. 9C). Of the nine abundantly expressed proteins readily identified by Coomassie blue staining that likely participate in contraction (48), three (filamin, MHC, and
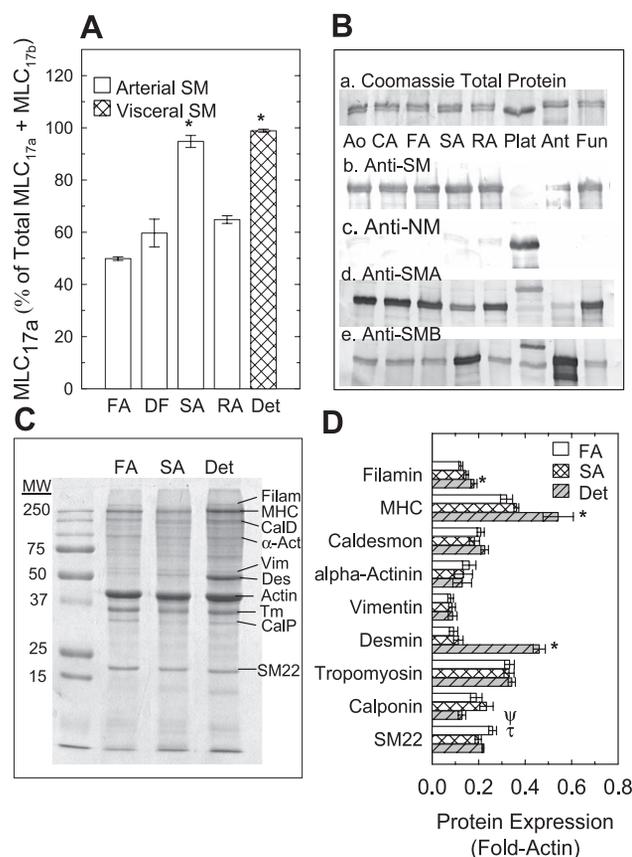

Fig. 9. *A*: essential MLC_{17} isoform expression levels for FA, DF, renal (RA), and SA arteries compared with visceral smooth muscle (SM). *B*: total protein (*Ba*) and relative levels of SM myosin (*Bb*), nonmuscle (NM) myosin (*Bc*), "slow" (SMA; *Bd*) and "fast" (SMB; *Be*) SM myosin heavy chain (MHC) isoforms for aorta (Ao), carotid artery (CA), FA, RA, SA, and visceral SM, stomach fundus (Fun), and antrum (Ant). Plat, rabbit platelet. *C* and *D*: comparison of expression levels of high-abundance proteins identified with Coomassie blue stain in FA, SA, and visceral Det (*C*, example of one gel and *D*, average values). Filam, filamin; CalD, caldesmon; α-Act, α-actinin; Vim, vimentin; Des, desmin; Tm, tropomyosin; CalP, calponin; SM22, 22-kDa SM-specific protein. Lanes in *C* were loaded with 10 μg protein. Protein bands in *C* were normalized in-lane to actin for quantification (*D*). Data in *A* and *D* are means ± SE ($n = 4$–5); *$P < 0.05$ compared with FA; Ψ$P < 0.05$ comparing Det to SA; τ$P < 0.05$ comparing Det and SA to FA. Data for *B* are examples derived from $n = 3$.

desmin) were expressed in greater abundance in the detrusor compared with FA and SA (Fig. 9D). Interestingly, detrusor expressed less calponin than SA ($P < 0.05$; Fig. 9D). Only 22-kDa smooth muscle-specific protein was expressed in increased abundance in the FA compared with SA and detrusor ($P < 0.05$; Fig. 9D), and no other of the nine proteins displayed differential expression when comparing SA to FA (Fig. 9D). These data together suggest that, overall, FA and SA were more similar than the SA and detrusor, despite the finding that, when considering motor protein expression, the SA and detrusor were more similar than SA and FA.

DISCUSSION

Results from the present study support the hypothesis that MLC phosphorylation and differential motor protein isoform expression determine the degree of developed sustained (tonic) isometric force in arterial smooth muscle. The elastic FA

expressed "slow" myosin isoforms and maintained relatively high KCl-induced levels of tonic MLC phosphorylation and force on stimulation with KCl, whereas the muscular SA expressed "fast" myosin isoforms and produced considerably weaker KCl-induced tonic levels of MLC phosphorylation and force. The most important finding was that SA, unlike its "parent" FA, did not appear to enter the latch state.

The mechanism of tonic force maintenance in the FA was very similar to that described for the carotid artery, another large elastic artery (5, 15, 33, 38). That is, maintenance of strong tonic forces in the face of falling levels of $[Ca^{2+}]_i$ and MLC phosphorylation in both FA and carotid artery can be ascribed to the formation of latch bridges. Latch bridges are proposed to impose an internal load against which rapidly cycling cross bridges must act (7), so the "trade-off" for permitting high force maintenance at a high energy economy [see review by Murphy (27)] is a reduced rate of muscle shortening (5, 7, 33). Whether latch bridges reflect an adaptation developed specifically to address the physiological requirements of all VSM or only of specific vascular segments is not known. However, visceral smooth muscles, such as the urinary bladder detrusor and stomach antrum that contract quickly and do not maintain high levels of tonic force, express "fast" myosin isoforms and display rapid actomyosin detachment rates, reflecting a lack of latch-bridge formation (9, 19, 46). We propose that low steady-state MLC phosphorylation levels and apparent absence of latch-bridge formation in the SA precluded its ability to maintain high levels of isometric force for the duration of a KCl-induced stimulation period.

The latch state provides a molecular explanation for maintenance of high VSM isometric stress in the face of falling levels of $[Ca^{2+}]_i$, MLC phosphorylation, and the maximum rate of cross-bridge cycling [see Dillon et al. (5), Dillon and Murphy (7), Hai and Murphy (15), and Murphy (27) for reviews]. As anticipated, a computer simulation of contraction based on the latch-bridge model demonstrated that MLC phosphorylation was not reduced enough by 5 and 10 min to permit a fall in stress in FA and SA. Rather, the latch-bridge model predicted that contraction should be maintained at high levels in SA and FA even when MLC phosphorylation fell from ~40 to ~28%. This is because a decrease in MLC phosphorylation from 40 to 20%, while reducing the fraction of phosphorylated, attached cross bridges, causes an increase in the fraction of dephosphorylated, attached cross bridges (i.e., latch bridges) (15). In fact, the signature feature of the latch-bridge model is that falling levels of MLC phosphorylation permit maintenance of high levels of force at a high energy economy by forming increased numbers of latch bridges [see Refs. 15 and 33 and also reviews by Murphy (27) and Murphy et al. (28)]. Thus the latch-bridge model predicts that, at steady state, SA should contain more latch bridges than FA because of a lower steady-state (tonic) level of MLC phosphorylation. However, if this were the case, then force redevelopment at steady state, a measure of cross-bridge cycling velocity (6), should be lower in SA than in FA, because a higher ratio of latch bridges-to-cycling (phosphorylated) cross bridges would impede cross-bridge cycling velocities (33). This was found not to be true. In fact, SA redeveloped force at a much higher rate than did FA, which is consistent with a report by Sherwood and Eddinger (43) that single smooth muscle cells isolated from SA shorten more rapidly than those isolated from FA. In short, the hypoth-

esis that the motor protein isoforms of SA formed latch bridges is not supported by our data showing that steady-state force fell nearly by half over a 5-min period from initiation of a KCl stimulus and that SA displayed much higher apparent cross-bridge cycling rates despite much lower levels of MLC phosphorylation than FA.

The lower levels of MLC phosphorylation produced by SA compared with FA could not be explained by a lower level of $[Ca^{2+}]_i$. Also, our data using inhibitors of MLC kinase and ROK suggest that additional MLC phosphorylation regulatory systems need not be invoked to explain the differential MLC phosphorylation values comparing FA and SA. Smooth muscle MLC phosphatase catalytic subunit is a PP1δ serine/threonine protein phosphatase isoform (20), and SA expressed nearly twofold more PP1δ than did FA. Moreover, SA expressed ~20% more MYPT-1, the regulatory subunit of MLC phosphatase. Thus one possible scenario is that, because of higher cellular levels of MLC phosphatase in SA compared with FA, the MLC phosphatase-to-kinase ratio was likewise elevated, reducing the steady-state level of MLC phosphorylation for a given $[Ca^{2+}]_i$. This hypothesis is supported by data obtained in permeabilized, Ca^{2+}-clamped tissues, suggesting that MLC phosphatase activity was approximately twofold greater in SA compared with FA.

There has been a great deal of speculation about the function of different MHC and MLC_{17} isoforms [see reviews by Arner et al. (2), Morano (26), and Ogut and Brozovich (29)], but a generally accepted model is that smooth muscles that display the phasic phenotype (fast contraction and weak tonic force maintenance) also display higher relative expression of "faster" myosin isoforms [i.e., SMB and MLC_{17a} compared with SMA and MLC_{17b}; see review by Arner et al. (2)]. Results from the present study support this hypothesis and provide evidence that expression of the "tonic" phenotype and latch-bridge formation is not a characteristic of all VSM. What remains to be determined is whether or not this hypothesis can be extended to blood vessels further down the vascular tree, or whether this conclusion is only valid for selected muscular arteries or selected vascular beds.

In conclusion, our data support a model whereby muscular arteries do not require expression of "slow" motor proteins and latch-bridge formation. Precisely why VSM of different segments of the vascular tree displays such dramatically different mechanical and regulatory behavior remains to be determined, but preliminary data from our laboratory (unpublished observations) support the view that latch bridges are an adaptation permitting constricted large-diameter arteries to temporarily resist full dilatation during increases in arterial pressures above the physiological resting level. Furthermore, these data support the speculative hypothesis that latch-bridge formation may not be a requirement of any blood vessels downstream from large elastic arteries, because of the absence of a physiological requirement to resist dilatation in blood vessels that normally can fully constrict to reduce luminal diameters even at very high pressures.

REFERENCES

1. **Aksoy MO, Williams D, Sharkey EM, and Hartshorne DJ.** A relationship between Ca^{2+} sensitivity and phosphorylation of gizzard actomyosin. *Biochem Biophys Res Commun* 69: 35–41, 1976.

2. **Arner A, Lofgren M, and Morano I.** Smooth, slow and smart muscle motors. *J Muscle Res Cell Motil* 24: 165–173, 2003.

3. **Butler TM, Mooers SU, Li C, Narayan S, and Siegman MJ.** Regulation of catch muscle by twitchin phosphorylation: effects on force, ATPase, and shortening. *Biophys J* 75: 1904–1914, 1998.

4. **Chacko S, Conti MA, and Adelstein RS.** Effect of phosphorylation of smooth muscle myosin on actin activation and Ca^{2+} regulation. *Proc Natl Acad Sci USA* 74: 129–133, 1977.

5. **Dillon PF, Aksoy MO, Driska SP, and Murphy RA.** Myosin phosphorylation and the cross-bridge cycle in arterial smooth muscle. *Science* 211: 495–497, 1981.

6. **Dillon PF and Murphy RA.** High force development and crossbridge attachment in smooth muscle from swine carotid arteries. *Circ Res* 50: 799–804, 1982.

7. **Dillon PF and Murphy RA.** Tonic force maintenance with reduced shortening velocity in arterial smooth muscle. *Am J Physiol Cell Physiol* 242: C102–C108, 1982.

8. **Eddinger TJ and Wolf JA.** Expression of four myosin heavy chain isoforms with development in mouse uterus. *Cell Motil Cytoskeleton* 25: 358–368, 1993.

9. **Fuglsang A, Khromov A, Torok K, Somlyo AV, and Somlyo AP.** Flash photolysis studies of relaxation and cross-bridge detachment: higher sensitivity of tonic than phasic smooth muscle to MgADP. *J Muscle Res Cell Motil* 14: 666–677, 1993.

10. **Gaylinn BD, Eddinger TJ, Martino PA, Monical PL, Hunt DF, and Murphy RA.** Expression of nonmuscle myosin heavy and light chains in smooth muscle. *Am J Physiol Cell Physiol* 257: C997–C1004, 1989.

11. **Giulian GG, Moss RL, and Greaser M.** Improved methodology for analysis and quantitation of proteins on one-dimensional silver-stained slab gels. *Anal Biochem* 129: 277–287, 1983.

12. **Greene LE and Sellers JR.** Effect of phosphorylation on the binding of smooth muscle heavy meromyosin X ADP to actin. *J Biol Chem* 262: 4177–4181, 1987.

13. **Grynkiewicz G, Poenie M, and Tsien RY.** A new generation of Ca^{2+} indicators with greatly improved fluorescence properties. *J Biol Chem* 260: 3440–3450, 1985.

14. **Hai CM and Murphy RA.** Regulation of shortening velocity by cross-bridge phosphorylation in smooth muscle. *Am J Physiol Cell Physiol* 255: C86–C94, 1988.

15. **Hai CM and Murphy RA.** Cross-bridge phosphorylation and regulation of latch state in smooth muscle. *Am J Physiol Cell Physiol* 254: C99–C106, 1988.

16. **Hai CM and Kim HR.** An expanded latch-bridge model of protein kinase C-mediated smooth muscle contraction. *J Appl Physiol* 98: 1356–1365, 2004.

17. **Herlihy JT and Murphy RA.** Length-tension relationship of smooth muscle of the hog carotid artery. *Circ Res* 33: 257–283, 1973.

18. **Hoar PE, Kerrick WG, and Cassidy PS.** Chicken gizzard: relation between calcium-activated phosphorylation and contraction. *Science* 204: 503–506, 1979.

19. **Horiuti K, Somlyo AV, Goldman YE, and Somlyo AP.** Kinetics of contraction initiated by flash photolysis of caged adenosine triphosphate in tonic and phasic smooth muscles. *J Gen Physiol* 94: 769–781, 1989.

20. **Ito M, Nakano T, Erdodi F, and Hartshorne DJ.** Myosin phosphatase: structure, regulation and function. *Mol Cell Biochem* 259: 197–209, 2004.

21. **Lee MR, Li L, and Kitazawa T.** Cyclic GMP causes Ca^{2+} desensitization in vascular smooth muscle by activating the myosin light chain phosphatase. *J Biol Chem* 272: 5063–5068, 1997.

22. **Lynn JA, Martin JH, and Race GJ.** Recent improvements of histologic technics for the combined light and electron microscopic examination of surgical specimens. *Am J Clin Pathol* 45: 704–713, 1966.

23. **Masuo M, Reardon S, Ikebe M, and Kitazawa T.** A novel mechanism for the Ca^{2+}-sensitizing effect of protein kinase C on vascular smooth muscle: inhibition of myosin light chain phosphatase. *J Gen Physiol* 104: 265–286, 1994.

24. **Mijailovich SM, Butler JP, and Fredberg JJ.** Perturbed equilibria of myosin binding in airway smooth muscle: bond-length distributions, mechanics, and ATP metabolism. *Biophys J* 79: 2667–2681, 2000.

25. **Mitsui T, Kitazawa T, and Ikebe M.** Correlation between high temperature dependence of smooth muscle myosin light chain phosphatase activity and muscle relaxation rate. *J Biol Chem* 269: 5842–5848, 1994.

26. **Morano I.** Tuning smooth muscle contraction by molecular motors. *J Mol Med* 81: 481–487, 2003.

27. **Murphy R.** Muscle cells of hollow organs. *News Physiol Sci* 3: 124–128, 1988.

28. **Murphy RA, Rembold CM, and Hai CM.** Contraction in smooth muscle: what is latch? *Prog Clin Biol Res* 327: 39–50, 1990.

29. **Ogut O and Brozovich FV.** Regulation of force in vascular smooth muscle. *J Mol Cell Cardiol* 35: 347–355, 2003.

30. **Patton C, Thompson S, and Epel D.** Some precautions in using chelators to buffer metals in biological solutions. *Cell Calcium* 35: 427–431, 2004.

31. **Paul RJ.** Smooth muscle energetics and theories of cross-bridge regulation. *Am J Physiol Cell Physiol* 258: C369–C375, 1990.

32. **Ratz PH and Murphy RA.** Contributions of intracellular and extracellular Ca^{2+} pools to activation of myosin phosphorylation and stress in swine carotid media. *Circ Res* 60: 410–421, 1987.

33. **Ratz PH, Hai CM, and Murphy RA.** Dependence of stress on cross-bridge phosphorylation in vascular smooth muscle. *Am J Physiol Cell Physiol* 256: C96–C100, 1989.

34. **Ratz PH.** High α_1-adrenergic receptor occupancy decreases relaxing potency of nifedipine by increasing myosin light chain phosphorylation. *Circ Res* 72: 1308–1316, 1993.

35. **Ratz PH.** Regulation of ERK phosphorylation in differentiated arterial muscle of the rabbit. *Am J Physiol Heart Circ Physiol* 281: H114–H123, 2001.

36. **Ratz PH, Meehl JT, and Eddinger TJ.** RhoA kinase and protein kinase C participate in regulation of rabbit stomach fundus smooth muscle contraction. *Br J Pharmacol* 137: 983–992, 2002.

37. **Ratz PH, Berg KM, Urban NH, and Miner AS.** Regulation of smooth muscle calcium sensitivity: KCl as a calcium-sensitizing stimulus. *Am J Physiol Cell Physiol* 288: C769–C783, 2005.

38. **Rembold CM and Murphy RA.** Myoplasmic calcium, myosin phosphorylation, and regulation of the crossbridge cycle in swine arterial smooth muscle. *Circ Res* 58: 803–815, 1986.

39. **Rembold CM and Murphy RA.** Latch-bridge model in smooth muscle: $[Ca^{2+}]_i$ can quantitatively predict stress. *Am J Physiol Cell Physiol* 259: C251–C257, 1990.

40. **Rhodin JAG.** Architecture of the vessel wall. In: *Handbook of Physiology. The Cardiovascular System. Vascular Smooth Muscle.* Bethesda, MD: Am. Physiol. Soc., 1980, sect. 2, vol. II, chapt. 1, p. 1–31.

41. **Sellers JR.** Mechanism of the phosphorylation-dependent regulation of smooth muscle heavy meromyosin. *J Biol Chem* 260: 15815–15819, 1985.

42. **Sellers JR, Spudich JA, and Sheetz MP.** Light chain phosphorylation regulates the movement of smooth muscle myosin on actin filaments. *J Cell Biol* 101: 1897–1902, 1985.

43. **Sherwood JJ and Eddinger TJ.** Shortening velocity and myosin heavy- and light-chain isoform mRNA in rabbit arterial smooth muscle cells. *Am J Physiol Cell Physiol* 282: C1093–C1102, 2002.

44. **Siegman MJ, Butler TM, Mooers SU, and Michalek A.** Ca^{2+} can affect V_{max} without changes in myosin light chain phosphorylation in smooth muscle. *Pflügers Arch* 401: 385–390, 1984.

45. **Somlyo AV, Khromov AS, Webb MR, Ferenczi MA, Trentham DR, He ZH, Sheng S, Shao Z, and Somlyo AP.** Smooth muscle myosin: regulation and properties. *Philos Trans R Soc Lond B Biol Sci* 359: 1921–1930, 2004.

46. **Szymanski PT, Chacko TK, Rovner AS, and Goyal RK.** Differences in contractile protein content and isoforms in phasic and tonic smooth muscles. *Am J Physiol Cell Physiol* 275: C684–C692, 1998.

47. **Urban NH, Berg KM, and Ratz PH.** K^+ depolarization induces RhoA kinase translocation to caveolae and Ca^{2+} sensitization of arterial muscle. *Am J Physiol Cell Physiol* 285: C1377–C1385, 2003.

48. **Weber LP, Seto M, Sasaki Y, Sward K, and Walsh MP.** The involvement of protein kinase C in myosin phosphorylation and force development in rat tail arterial smooth muscle. *Biochem J* 352: 573–582, 2000.

49. **Wingard CJ, Paul RJ, and Murphy RA.** Energetic cost of activation processes during contraction of swine arterial smooth muscle. *J Physiol* 501: 213–223, 1997.

50. **Yu SN, Crago PE, and Chiel HJ.** A nonisometric kinetic model for smooth muscle. *Am J Physiol Cell Physiol* 272: C1025–C1039, 1997.